Phys Chem Minerals (2001) 28: 67–75

ORIGINAL PAPER

M. Iglesias · K. Schwarz · P. Blaha · D. Baldomir

Electronic structure and electric field gradient calculations of Al_2SiO_5 polymorphs

Received: 22 March 2000 / Accepted: 3 August 2000

Abstract The electronic structure of the three polymorphs of Al_2SiO_5, andalusite, sillimanite, and kyanite, is studied by linearized-augmented-plane-wave (LAPW) calculations using the WIEN code. Total energy calculations verify, in agreement with recent pseudopotential calculations, that andalusite is the most stable phase, followed by sillimanite and kyanite.We determine the electronic charge density distribution and find strong polarizations on all oxygen ions. We identify different polarizations due to Al or Si neighbors which depend on their respective distances to the oxygen atom. The chemical bonding is not purely ionic in nature but has important covalent contributions. Electric field gradients (EFGs) at all sites are calculated and agree well (within 10%) with available experimental data on Al. We identify the origin of the EFGs and demonstrate its relation to the nearest-neighbor coordination and the resulting anisotropy of the electronic charge distribution.

Key words Andalusite · Sillimanite · Kyanite · EFG tensor · Charge distribution

Introduction

Andalusite, sillimanite and kyanite are three polymorphs of Al_2SiO_5 that commonly appear in metamorphosed pelitic sediments. Apart from their importance in the fields of metamorphic and experimental petrology, they are also interesting from the crystal-chemical point of view since Al occurs in these systems in three different coordinations, namely four-, five-, and six-fold coordinated in sillimanite, andalusite, and kyanite, respectively. Therefore, a detailed study of the electronic structures of these aluminum silicates is important in order to understand their relative stability and the bonding mechanism.

Many experimental studies have been devoted to the determination of the crystal structure and other properties of these minerals. For a comprehensive review see the book by Kerrick (1990) and references therein.

The electric-field gradient (EFG) is a ground-state property of a solid and depends sensitively on the asymmetry of the electronic charge density near the probe nucleus in a crystal. EFGs are measured with nuclear magnetic resonance (NMR), nuclear quadrupole resonance (NQR) or Mössbauer spectroscopy. In the case of Al_2SiO_5, the nuclear quadrupole coupling tensors have been determined from NMR experiments for ^{27}Al in andalusite by Hafner et al. (1970), in sillimanite by Raymond and Hafner (1970), and in kyanite by Hafner and Raymond (1967). Alemany et al. (1991) have measured these coupling tensors for both andalusite and kyanite and very recently Bryant et al. (1999) performed NMR measurements on single crystals of andalusite.

For a long time EFGs have been explained by point-charge models (PCM). These predictions, however, depend on empirical parameters like atomic charges or Sternheimer antishielding factors, and their results often deviate significantly from experimental data. Hafner and Raymond (1967) applied the PCM to kyanite, and later Raymond (1971) extended this study to all three Al_2SiO_5 polymorphs using the point-multipole method. These studies led to two different assignments for the four aluminum sites in kyanite, and Raymond's (1971) results still deviate by up to 25% from the experimental values, although he used different sets of empirical parameters for the three systems. This calls for an ab initio determination of the EFGs in these three polymorphs.

M. Iglesias (✉) · D. Baldomir
Física Aplicada, Universidade de Santiago de Compostela,
15706 Santiago de Compostela, Spain
e-mail: famoises@usc.es

K. Schwarz · P. Blaha
Institute of Physical and Theoretical Chemistry,
Vienna University of Technology, A-1060 Vienna,
Getreidemarkt 9/156, Austria

Blaha et al. (1985) developed a first-principles method to compute EFGs from an all-electron band-structure calculation. In this approach the linearized augmented plane-wave (LAPW) method was used and the EFG was calculated directly from the self-consistent charge density. Since the first results on the superionic conductor Li_3N (Blaha et al. 1985), this method has been successfully applied to a variety of systems like the hcp metals up to Cd (Blaha et al. 1985, 1988), the high T_c superconductor (Schwarz et al. 1990), several Fe compounds (Dufek et al. 1995) or minerals (Winkler et al. 1996).

In the present work we performed LAPW calculations for the three polymorphs and studied the relative stability by total energy calculations and the electronic structure using partial densities of states, EFGs, the electron density distributions and their anisotropies. During preparation of this manuscript we learned about a recent paper by Bryant et al. (1999), who calculated the EFG tensor on the two Al sites in andalusite using both the LAPW method and a Hartree-Fock cluster approach. They discuss the reliability of these methods, but provide no interpretation for the origin of the EFG. The main goal of the present paper is to explain the relation between EFG tensor and charge distribution, chemical bonding, and structural aspects.

Structures

The structural parameters for the three polymorphs have been taken from Ralph et al. (1984) for andalusite, from Yang et al. (1997a) for sillimanite, and from Yang et al. (1997b) for kyanite. In all cases the structures refined at ambient conditions were used.

All three polymorphs have 32 atoms per unit cell ($Z = 4$), andalusite and sillimanite are orthorhombic with space group *Pnnm* and *Pbnm*, respectively, and kyanite is triclinic with space group $P\bar{1}$. This leads to 7 non-equivalent atoms in andalusite and sillimanite (with two different aluminum sites) and 16 nonequivalent atoms in kyanite (with four different aluminum sites). In all three cases the structure consists of chains of octahedrally coordinated aluminum atoms parallel to the *c* axis sharing edges with alternating silica tetrahedra and polyhedra of aluminum in fourfold (sillimanite), fivefold (andalusite), or sixfold (kyanite) coordination.

Detailed representations of the structures, projections, and positional parameters of the atoms can be found in the references given above. Here we just show (Fig. 1) the local coordination around the Al_1 site in andalusite. Al_1 has relatively short bonds to O_a and O_b (see Table 1) but a significantly longer one to the apical O_d, indicated by the diameter of the sticks of the ball and stick model shown in Fig. 1. O_a and O_b are both connected to Al_1 (of the edge-shared next octahedron) but

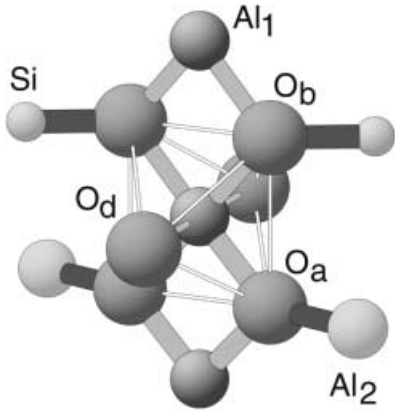

Fig. 1 Local arrangement of the atoms in andalusite in the vicinity of Al_1, which is octahedrally coordinated by two O_a and O_b (basal plane) and two O_d (apical) oxygen atoms, that are linked to Al_2, Si, and Si and Al_2 in the next coordination shell. Shorter bond distances are indicated by *thicker sticks*

on the other side O_a is bound to Al_2 whereas O_b forms a bond with Si. The other oxygen atom of the octahedron, O_d, is connected both with Al_2 and Si. This strong deviation from the perfect octahedron and the different coordinations in the next shell will be important for our analysis of the EFG. For a further discussion of the structural features of all three polymorphs the reader is referred to Winter and Ghose (1979), Ralph et al. (1984), and Yang et al. (1997a, b).

Computational detailsz

We calculate the electronic structure utilizing the well-known full-potential LAPW method, in which no shape approximation, either on the potential or on the electronic charge density, is made, and use the WIEN code (Blaha et al. 1999). The exchange and correlation effects are treated in the density functional theory (DFT) with both the local density approximation (LDA) (Perdew and Wang 1992) and the generalized gradient approximation (GGA) (Perdew et al. 1996).

We have taken the following sphere radii for the calculations: 1.8 a.u. for Al, 1.5 a.u. for Si, and 1.4 a.u. for O. A plane wave cut-off of $R_{mt}K_{max} = 6.75$, where R_{mt}, the smallest of all atomic sphere radii, is used for the three polymorphs leading to more than 4000 LAPWs in our basis set. In additional calculations we checked that the results are well converged for these cutoff values (see also Bryant et al. 1990). The Al 2*p*, Si 2*p*, and O 2*s* orbitals lie between −100 and −10 eV and their charges are not completely confined inside the respective atomic spheres. Therefore we treat these semicore states by employing additional local orbitals (Singh 1991). We used 36 *k* points in the irreducible Brillouin zone (IBZ) for andalusite and sillimanite and 40 *k* points for kyanite. All the cases were studied by nonspin-polarized calculations.

Table 1 Space groups and interatomic distances (in Å) for andalusite, sillimanite, and kyanite

Andalusite (*Pnnm*)		Sillimanite (*Pbnm*)		Kyanite ($P\bar{1}$)			
Atoms	Distance	Atoms	Distance	Atoms	Distance	Atoms	Distance
Al_1 O_a(2x)	1.827	Al_1 O_b(2x)	1.869	Al_1 O_9	1.848	Al_4 O_1	1.816
O_b(2x)	1.891	O_a(2x)	1.915	O_{10}	1.850	O_2	1.846
O_d(2x)	2.086	O_d(2x)	1.956	O_2	1.873	O_8	1.874
				O_6	1.885	O_4	1.909
Al_2 O_d(2x)	1.814	Al_2 O_c	1.709	O_7	1.972	O_5	1.934
O_a	1.816	O_b	1.747	O_8	1.986	$O_{1'}$	1.995
O_c	1.839	O_d(2x)	1.796	Al_2 O_3	1.881	Si_1 O_4	1.631
O_c	1.899			O_4	1.890	O_8	1.622
				O_6	1.910	O_5	1.642
Si O_c	1.618	Si O_c	1.569	O_{10}	1.922	O_{10}	1.645
O_d(2x)	1.630	O_a	1.636	O_9	1.929	Si_2 O_7	1.624
O_b	1.645	O_d(2x)	1.644	O_2	1.937	O_3	1.629
				Al_3 O_5	1.860	O_1	1.640
				O_6	1.881	O_9	1.646
				O_7	1.885		
				O_3	1.924		
				$O_{6'}$	1.969		
				O_2	1.984		

Stability

Since the complete optimization of a structure containing 32 atoms per unit cell is quite expensive from the computational point of view for the highly accurate LAPW method, the experimental parameters have been used directly in our calculations. In order to check how far we are from the equilibrium parameters and how well our calculations reproduce the experimental structural parameters, we have calculated the forces acting on all atoms. Except for O_c in sillimanite, where the force is $\sim$21 mRy/a.u., all forces are less than 15 mRy/a.u., a relatively small value, which would cause bond distances to relax by less than 1%. We have tested this by optimizing the internal atomic positions in andalusite keeping the lattice parameters fixed. This optimization led to slightly longer distances in all bonds except for the longest bond (Al_1-O_d), which is 1% smaller, making the octahedron a little less distorted. The energy for the relaxed positions was only 12 meV/f.u. lower than for the experimental positions, a value that is much smaller than the energy separation between the three polymorphs (see below). Note that we used the experimental lattice constants and made no attempt to minimize the energy with respect to the unit cell dimensions. Nevertheless, we can assume that the structures are almost relaxed, so that we can use our results to analyze the theoretical stability of these polymorphs.

In the GGA treatment for exchange and correlation, which often is more reliable for total energy calculations than LDA, andalusite is the ground state and thus the most stable polymorph, whereas sillimanite lies 0.08 eV/f.u. and kyanite 0.14 eV/f.u. higher than the ground state of andalusite. These GGA results are in good agreement with recent pseudopotential calculations (Oganov et al. 2000), but in contrast to experiment (Olbricht et al. 1994) which finds kyanite to be more stable by 0.04 eV/f.u. than andalusite, and the latter 0.04 eV/f.u. more stable than sillimanite. Calculations using the less accurate LDA yield qualitatively the correct ordering, but the energy differences are significantly overestimated, since andalusite lies 0.18 eV/f.u. and sillimanite 0.32 eV/f.u. higher than kyanite.

The electronic structure

The electronic structure has been calculated by the LAPW method for the three polymorphs and provides the basis for the following results and interpretations. The band structure consists of low-lying bands originating from the O-2*s* states at about 16–20 eV below the top of the valence band, which is taken to be at 0. The valence bands have a width of about 8 eV and the conduction bands are separated by a gap of 5.2, 5.5, and 6.3 eV for andalusite, sillimanite, and kyanite, respectively. Note that gaps are underestimated in DFT calculations and often have about half the experimental value.

Since the cross-features of the density of states (DOS) are rather similar for all the atoms in all three polymorphs, we take andalusite as a representative example below. The total valence DOS can be decomposed into local (inside the atomic sphere) partial (*l*-like) DOS according to the LAPW method, in which a corresponding representation of the wavefunction is used. Figure 2 shows the partial DOS for the valence band region, which consists of mainly O-2*p*, Al-3*s* and -3*p*, and Si-3*s* and -3*p* contributions. The Si states are at somewhat lower energies and the *s*-*p* splitting is more pronounced than for the corresponding Al states. All these five orbitals are strongly mixed over the entire valence band region. Small details of the various interactions determine the properties described next.

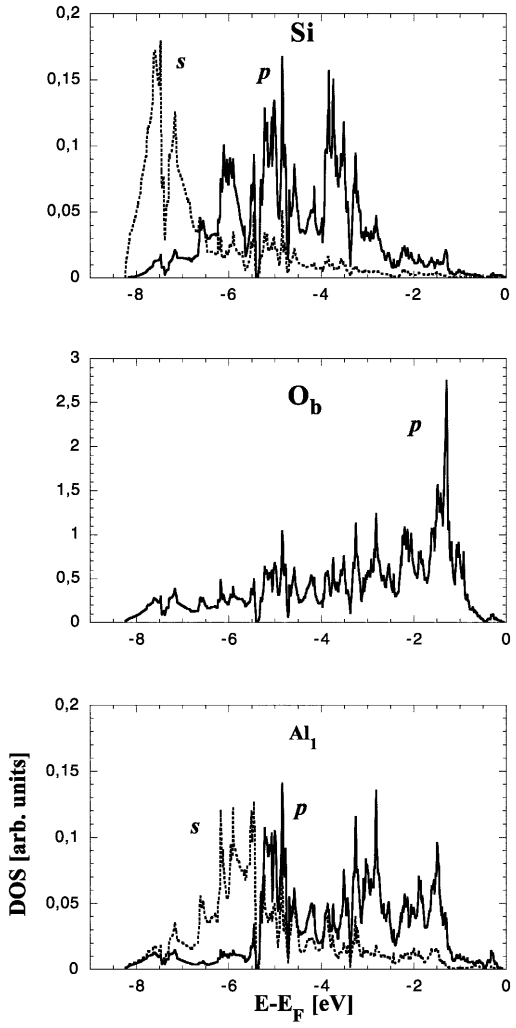

Fig. 2 Partial site and *l*-decomposed DOS of the valence bands in andalusite

Electric field gradients

Method

A nucleus with a nuclear-spin quantum number $I \geq 1$ has a nuclear quadrupole moment (Q) that can interact with the electric field gradient (EFG) which originates from the (nonspherical) charge distribution surrounding this nucleus. This interaction determines the nuclear quadrupole coupling constant eQV_{zz}/h, where V_{zz} is the principal component of the EFG tensor, e is the electric charge and h is Planck's constant. The EFG is defined as the second derivative of the electrostatic potential at the nuclear position written as traceless tensor.

Blaha et al. (1985) have developed a first-principles method to calculate EFGs directly from the self-consistent charge density by solving Poisson's equation without further approximations. In this method no assumption is made on the charge distribution and there is no need for Sternheimer antishielding factors (often derived from free atoms) which should describe core polarization effects. A detailed explanation of the formalism and additional references can be found in Schwarz et al. (1990). Diagonalization of the EFG tensor yields the eigenvalues and principal axes. Following Blaha et al. (1985), we use the standard convention

$$|V_{zz}| \geq |V_{yy}| \geq |V_{xx}| \ , \tag{1}$$

according to which the EFG tensor is characterized by the principal component V_{zz} and the asymmetry parameter η, given by

$$\eta = \frac{V_{xx} - V_{yy}}{V_{zz}} \ , \tag{2}$$

where η varies between 0 (axial symmetry) and 1 ($V_{xx} = 0$).

The EFG is sensitive to the anisotropy in the charge density around the corresponding nucleus and thus can be related to the symmetry-decomposed partial charges, as was shown in Schwarz et al. (1990), where Δn_p is an anisotropy count in terms of partial charges. For the elements in the present cases the main contribution to the EFG comes from the p orbitals and this relation reads:

$$V_{zz}^{p} \approx \Delta n_p \left\langle \frac{1}{r^3} \right\rangle_p \tag{3}$$

$$\Delta n_p = \frac{1}{2}(p_x + p_y) - p_z \ , \tag{4}$$

and $\left\langle \frac{1}{r^3} \right\rangle_p$ is the expectation value of the corresponding p orbitals. The anisotropy from the d-orbitals can be neglected for the present elements.

Results

In the Al_2SiO_5 polymorphs, Al appears with different coordinations and symmetries. In andalusite and sillimanite there are two, in kyanite four symmetrically inequivalent aluminum sites. In Table 2 our calculated Al EFGs and their asymmetry parameters are compared to the experimental data from Raymond and Hafner (1970) and from Alemany et al. (1991). In Table 3 we include EFGs and η values for Si and O although, to the best of our knowledge, no experimental data are available for these atoms in any of the polymorphs. A table with the full EFG tensors (with respect to the crystal axes) is available from the authors[1]. Since the EFGs calculated within LDA or GGA differ very little, we show and discuss only the GGA results. In the experimental studies an ambiguity remains in the sign of the eigenvalues, since only the magnitude of EFGs was reported. A value of $Q = 0.140b$, taken from Pyykkö (1992), was used for ^{27}Al in the conversion from NMR frequencies to EFGs. Good agreement is found between our calcu-

[1] The full EFG tensors can be obtained from: kschwarz@theochem.tuwien.ac.at

Table 2 Theoretical and experimental EFGs (in 10^{21} V m^{-2}) and asymmetry parameters for Al atoms in andalusite, sillimanite and kyanite

		Andalusite		Sillimanite		Kyanite	
		Theory	Expt.[a]	Theory	Expt.[b]	Theory	Expt.[c]
Al_1	EFG	+4.11	4.51	−2.32	2.63	+2.66	2.96
	η	0.08	0.10	0.49	0.46	0.26	0.27
Al_2	EFG	+1.57	1.72	−1.82	2.00	−0.96	1.09
	η	0.73	0.67	0.51	0.53	0.84	0.89
Al_3	EFG					−1.75	1.93
	η					0.64	0.59
Al_4	EFG					−2.51	2.77
	η					0.39	0.38

[a] Bryant et al. (1999)
[b] Raymond and Hafner, (1970)
[c] Alemany et al. (1991)

lated values and the experimental data (∼10%) for all aluminum sites in the three systems (Table 2). It is, however, striking that our theoretical EFGs are constantly too small by about 11%. This (and the very good agreement for η, see below) suggests a possible larger value for the nuclear quadrupole moment Q of ^{27}Al. If we used only a slightly larger value for Q, namely $Q = 0.155b$, all EFGs would be within 3% of the experimental data. However, one should verify this suggestion by EFG calculations for other Al compounds with different kind of bonding, to make sure that this is not a result of a systematic LDA error in the description of the Al-O bonding. Such a study was made with great success for determining Q of ^{57}Fe (Dufek et al. 1995).

It should be mentioned that our results for the Al-EFGs in andalusite are in very good agreement with the recent calculations by Bryant et al. (1999), in both magnitude and direction for all tensor components. They employed the identical computer code (Blaha et al. 1999) but used slightly different structural parameters, which are responsible for the small differences. This demonstrates again the reliability of such LAPW calculations.

Table 3 Theoretical EFGs (in 10^{21} V m^{-2}) and asymmetry parameters for Si and O atoms in andalusite, sillimanite, and kyanite

Andalusite			Sillimanite			Kyanite		
Atom	EFG	η	Atom	EFG	η	Atom	EFG	η
Si	+1.99	0.48	Si	−1.93	0.17	Si_1	+0.93	0.64
						Si_2	+1.11	0.39
O_a	−4.59	0.18	O_a	−5.81	0.67	O_1	+6.96	0.74
O_b	−5.84	0.83	O_b	−5.11	0.01	O_2	+3.78	0.81
O_c	+3.97	0.85	O_c	+6.38	0.08	O_3	−6.22	0.89
O_d	−6.68	0.51	O_d	−6.94	0.52	O_4	−6.29	0.96
						O_5	+6.48	0.93
						O_6	+3.00	0.83
						O_7	−6.45	0.73
						O_8	−6.26	0.71
						O_9	−6.48	0.89
						O_{10}	−6.49	0.87

Early PCM calculations for kyanite by Hafner and Raymond (1967) suggested an EFG assignment to the four aluminum sites different from in the present work. Raymond's (1971) point-multipole method found the same assignment as we did, but his results deviate up to 25% from the experimental values although different sets of empirical parameters were used for the three systems. This is in contrast to our approach, which is completely based on an ab initio methodology.

An important goal of the present work is to analyze the origin of the EFG. First, we divide the total EFG into contributions from the semicore (these are states originating from Al 2*p* and O 2*s* orbitals) and the real valence states (Al 3*s*, 3*p*, O 2*p*, and Si 3*s*, 3*p*). In all cases, the main contribution to the EFG comes from the distortion from spherical symmetry of the respective valence p electrons. Even a slightly different occupation of p_x, p_y, and p_z orbitals due to polarization effects and chemical bonding with neighboring atoms has a dominant effect on the EFG. The low-lying Al 2*p* semicore states contribute less than 25% to the total Al EFG, whereas an important fraction of the Si EFG (up to 50%) originates from the O 2*s* semicore states, which enter the Si atomic sphere due to very short Si-O bond distances.

In the following we demonstrate for a few examples the relation between EFGs, chemical bonding, and the nearest-neighbor Al-O coordination.

In Fig. 1 the highly distorted octahedron around the Al_1 atom in andalusite is displayed. As described above, the distances (Table 1) between Al_1 and four oxygens are rather similar (Al_1-O_a = 1.827 Å, Al_1-O_b = 1.891 Å) while the distance to the other two apical oxygen atoms is much larger (Al_1-O_d = 2.086 Å). This corresponds to a large distortion of the octahedron with an elongation in the direction O_d-Al_1-O_d, which leads to a smaller Al_1 *p*-like charge (towards the O_d atoms), as will be shown later in the electron density plots (Fig. 3) or the partial charges (Table 4). Consequently, the principal axis of the EFG tensor (Table 2) lies in the O_d-Al_1-O_d direction. A significantly smaller p_z charge leads to a large positive asymmetry count Δn_p [Eq. (4)] and thus to a positive EFG [Eq. (3)], which is the largest Al EFG in all three systems due to the strongest distortion. On the other hand, the Al_2 site in kyanite has the least distorted octahedron, since the Al-O distances differ by less than 3% (1.881–1.937 Å, Table 1). Therefore, it has the smallest EFG of all Al sites in these three compounds. We thus can make the general statement that the Al-EFG in an octahedral environment depends sensitively on distortions (cf. Tables 1 and 2).

The asymmetry parameter η does not depend on Q and thus the perfect agreement between our results and experiment is rather convincing (Table 2). Again, a clear connection between η and the nearest-neighbor coordination can be established: for instance, there is a clear difference in the η parameter for the octahedral (Al_1) site between andalusite and sillimanite which can easily be explained. In andalusite the Al_1 site has point symmetry

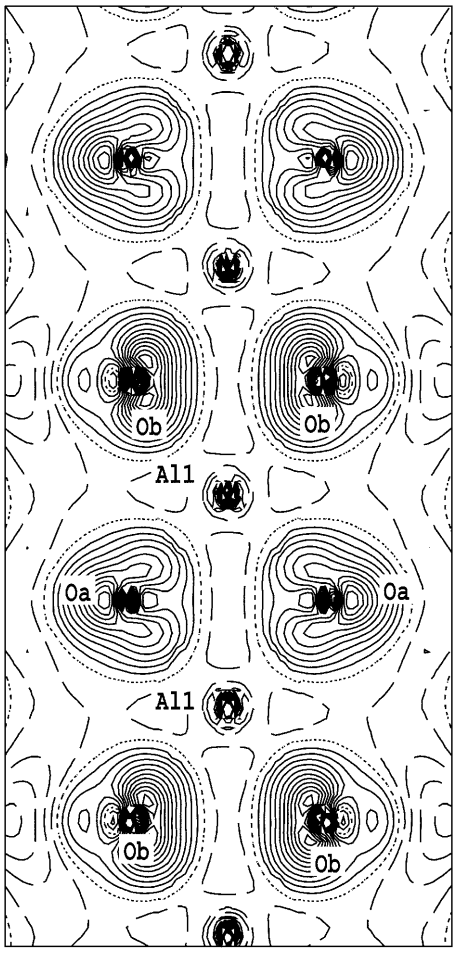

Fig. 3 Difference electron density $\Delta\rho$ of andalusite in the basal plane of the edge-share Al_1 octahedra. *Solid*, *dotted* and *dashed lines* correspond to positive, zero and negative $\Delta\rho$ respectively. The *contour intervals* are in units of 0.05 $e\text{Å}^{-3}$

m and thus one direction of the EFG tensor is fixed to be parallel to the crystallographic c direction. As described above, the principal component of the Al_1 EFG tensor points into the O_d-Al_1-O_d direction (Fig. 1), and forms 29° with the crystallographic *a* axis. The other components must lie approximately in the basal plane of the octahedron (O_a-O_b-O_b-O_a), with V_{yy} along the c direction (between O_b-O_b, fixed by symmetry) and V_{xx} normal to it between O_b-O_a (see Fig. 1). The charge distribution along those *x* and *y* directions is rather similar (see Fig. 3), producing a small value of η. The interpretation of sillimanite is not as simple, since the oxygen-octahedron is distorted in a more complicated way and its site symmetry is reduced to $\bar{1}$. Therefore, no EFG direction is fixed by symmetry. The main component of the EFG does not lie in the O_d-Al_1-O_d direction (the longest Al-O distances) but is tilted and η is large. A similar analysis holds of course, also for oxygen. For instance, in sillimanite O_b has an almost coplanar triangular Al_1-Al_2-Al_1 environment, leading to a negative EFG perpendicular to that plane and an almost axial EFG ($\eta = 0.01$), while O_c is nearly linearly coordinated by one Si and one Al_2 atom and the positive EFG points in this direction with nearly axial symmetry.

It is, of course, not always possible to interpret the EFG in such a simple way. Sometimes several competing effects, which may even partially cancel each other, complicate the analyses.

Charge distribution

Anisotropy

Figures 3–5 show some difference electron densities $\Delta\rho$ for andalusite. $\Delta\rho$ represents the difference between the crystalline electron density and the superposed electron densities of the neutral atoms. In these figures negative lines represent those places where the electron density is lower in the crystal than for the superposition of neutral atoms (e.g., the positively charged Al ions), while positive regions indicate the negative oxygen ions. This charge transfer, however, does not correspond to a

Table 4 Total charges inside the atomic spheres for the three polymorphs

Andalusite			Sillimanite			Kyanite		
Atom	Charge	Av. dist.	Atom	Charge	Av. dist.	Atom	Charge	Av. dist.
Al_1	6.625	1.935	Al_1	6.613	1.913	Al_1	6.656	1.902
Al_2	6.672	1.836	Al_2	6.729	1.762	Al_2	6.618	1.912
						Al_3	6.623	1.917
						Al_4	6.660	1.896
Si	6.718	1.631	Si	6.726	1.623	Si_1	6.710	1.635
						Si_2	6.709	1.635
O_a	4.629	1.823	O_a	4.646	1.822	O_1	4.653	1.817
O_b	4.646	1.809	O_b	4.623	1.828	O_2	4.630	1.910
O_c	4.676	1.765	O_c	4.668	1.639	O_3	4.651	1.811
O_d	4.636	1.843	O_d	4.651	1.799	O_4	4.653	1.810
						O_5	4.650	1.812
						O_6	4.625	1.911
						O_7	4.645	1.827
						O_8	4.649	1.824
						O_9	4.649	1.807
						O_{10}	4.650	1.806

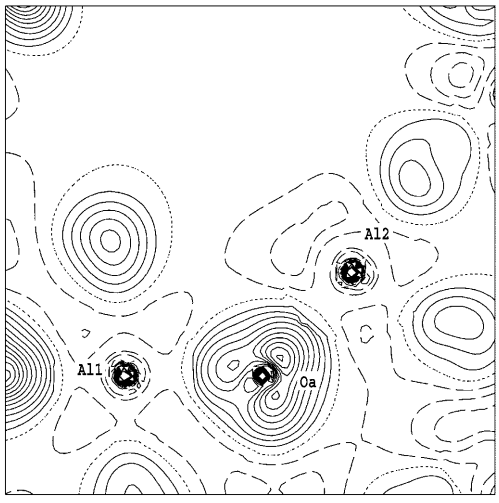

Fig. 4 Difference electron density $\Delta\rho$ in the plane of Al_1-O_a-Al_2 in andalusite. (Details as in Fig. 3)

purely ionic bond, since the charge density around the oxygen atoms is by no means spherical, but is highly polarized.

Figure 3 shows the difference density in the O_a-Al_1-O_b plane of andalusite, where the high polarization of the charge density of the oxygens atoms towards aluminum is clearly displayed. The differences between the electronic clouds of O_a and O_b are due to the local connections they have with their nearest neighbors (Fig. 1). O_a has three aluminum neighbors and thus its charge density is concentrated along these three bonds, as shown in Fig. 4, whereas in O_b the charge is depleted in the direction O_b-Si and is polarized towards the Al_1 atoms (see Fig. 5). Figures 4 and 5 clearly display the links between the different polyhedra. While O_a takes part in the connection between Al_1 octahedra and Al_2 polyhedra, O_b contributes to link Al_1 octahedra and Si tetrahedra. Some of these relations can be seen in Fig. 1.

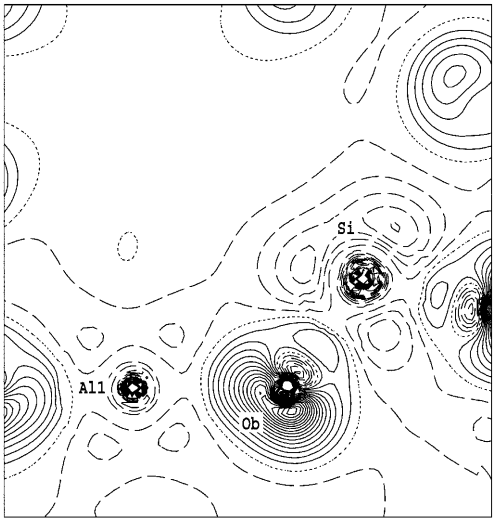

Fig. 5 Difference electron density $\Delta\rho$ in the plane of Al_1-O_b-Si in andalusite. (Details as in Fig. 3)

If we analyze our results, we find a general tendency of the oxygen atoms to concentrate their electron density in the direction of the longer O-Al bonds whereas in the shorter O-Si bond direction a strong reduction of the positive difference density was found (Figs. 3, 5). This fact will be discussed further below. The tendency to accumulate oxygen charge density towards aluminum atoms occurs in all three polymorphs when an oxygen atom is connected to both Si and Al. In cases where oxygen is not connected to silicon (O_a in andalusite and O_2, O_6 in kyanite), the charge density is lower towards those Al atoms which are further away (Fig. 4). Another special case is O_c in sillimanite, which is connected to only to one Si and one Al_2 atom, and shows a depletion of charge in the (short) O_c-Si bond and an increased density in the direction O_c-Al_2.

The observations made above can be explained by simple molecular-orbital (MO) arguments, but due to the complicated structural relations, a complete MO picture is not possible in these silicates. The short Si-O bonds have, of course, the largest bonding-antibonding splitting, and thus the corresponding antibonding states are partially unoccupied leading to a reduced $\Delta\rho$ in these bonding directions. The longer Al-O bonds show much less bonding-antibonding splitting, and thus more of the antibonding states are occupied, leading to a larger $\Delta\rho$. Thus, we want to stress that the small positive $\Delta\rho$ between O and Si corresponds to the stronger covalent bond, while the larger positive $\Delta\rho$ between O and Al corresponds to a more ionic bond. Similar features were also discussed in the high T_c materials for Cu-O bonds by Schwarz et al. (1990) and Ambrosch-Draxl et al. (1991).

Total charges inside the spheres

In the LAPW formalism space is partitioned in two types of regions, namely the spheres around the atoms and the interstitial region, where different basis set expansions are used. Inside the atomic spheres this expansion is made with atomic-like solutions of Schrödinger's equation whereas in the interstitial region plane waves are used. Due to this spatial decomposition, part of the electronic charge falls in the interstitial region, where it can not be assigned to a particular atom. Partition of charge into partial charges is not unique and is always model-dependent. Note that the given charges within the atomic spheres are not comparable to usual ionic charges. Nevertheless, the electronic charge inside the spheres surrounding the atomic nucleus can be helpful to discuss trends, bond properties, and charge transfer between the atoms, especially when the same sphere radius is used in different compounds.

Table 4 presents total charges inside the spheres for all the atoms in the three systems and the average distance to the neighboring atoms. We can see that, in

general, larger distances lead to smaller charges inside the sphere. As explained in the last section, longer distances lead to more oxygen charges in these directions and, therefore, more interstitial charge, producing a decrease in the charges inside the sphere. However, some cases require special explanations. For example, the asymmetry of the charge density around O_a in andalusite does not follow this trend and a larger total charge is found inside the sphere than expected from the distances. This behavior is due to the fact that O_a has no Si nearest neighbor, in contrast to the other oxygens. In kyanite, all the oxygens except O_2 and O_6 have rather similar distances and thus only small differences are expected for the respective charges inside the spheres, whereas O_2 and O_6 are at longer distances and thus their spheres contain smaller charges. We should also mention that Al_3 in kyanite deviates from the general trend of charge accumulation according to distance, since it has a slightly larger charge than Al_2 although its average distance is longer. The reason for this is that Al_3 is connected to three oxygens with smaller charges (O_2 and two O_6), whereas all the other Al are connected to two or less of such oxygens which transfer part of their charge to aluminum.

Summary

We performed electronic structure calculations for the three polymorphs of Al_2SiO_5, andalusite, sillimanite, and kyanite. We find, in agreement with recent theoretical work, but in disagreement with experiment, that andalusite is the most stable phase, followed by sillimanite and kyanite, when we use the more advanced GGA approximation for exchange and correlation effects, whereas the less accurate LDA calculations would predict kyanite as the most stable form, but with largely overestimated energy differences.

The electronic structure and chemical bonding is discussed using an analysis of partial charges and charge densities and significant covalent contributions are found. Difference electron densities show a highly polarized positive difference density around oxygen. This oxygen density shows an increase in the direction of Al neighbors, whereas the O charge is depleted towards Si neighbors. It should be stressed that this depletion is caused by a strong covalent Si-O bond for which antibonding states are partially shifted above E_F and consequently less O charge is found towards the Si neighbors. The valence band width is about 8 eV and the conduction bands are separated by a gap of 5–6 eV.

The EFG on all Al sites agrees well with experiment and thus our assignment of the experimental frequencies to the different crystallographic Al sites is unambiguous In addition, we made predictions for the EFG at all O sites. We have given a detailed explanation of the origin of the EFG, which stems mainly from an anisotropy of the Al 3*p* charge due to chemical bonding with the neighboring O atoms. The connection between EFG tensor and nearest-neighbor environment has been demonstrated for selected examples.

Acknowledgements We are grateful to Prof. S. Ghose, who suggested this study, and to Dr. B. Winkler for his valuable discussions. One of us (M.I.) would like to thank the Universidade de Santiago de Compostela and Xunta de Galicia for the financial support. He also wants to thank for the hospitality he has received during his stay at the Technische Universität Wien, where most of the work was done. P.B. was supported by the Austrian Science Foundation (P13430-PHY).

References

Alemany LB, Massiot D, Sherriff BL, Smith ME, Taulelle F (1991) Observation and accurate quantification of ^{27}Al MAS NMR spectra of some Al_2SiO_5 polymorphs containing sites with large quadrupole interactions. Chem Phys Lett 177: 301–306

Ambrosch-Draxl C, Blaha P, Schwarz K (1991) Electronic structure and electric-field gradients for $YBa_2Cu_4O_8$ from density-functional calculations. Phys Rev B 44: 5141–5147

Blaha P, Schwarz K, Herzig P (1985) First-principles calculation of the electric field gradient of Li_3N. Phys Rev Lett 54: 1192–1195

Blaha P, Schwarz K, Dederichs PH (1988) First-principles calculation of the electric-field gradient in hcp metals. Phys Rev B 37: 2792–2796

Blaha P, Schwarz K, Luitz (1999) WIEN97 A full potential linearized augmented plane wave package for calculating crystal properties, Karlheinz Schwarz, Techn. Universität Wien, Austria ISBN 3-9501031-0-4 (An improved version of Blaha P, Schwarz K, Sorantin P, Trickey SB (1990)) Comp Phys Commun 59: 399

Bryant PL, Harwell CR, Wu K, Fronczek FR, Hall RW, Butler LG (1999) Single-crystal ^{27}Al NMR of andalusite and calculated electric field gradients: the first complete NMR assignment for a 5-coordinate aluminum site. J Phys Chem A 103: 5246–5252

Dufek P, Blaha P, Schwarz K (1995) Determination of the nuclear quadrupole moment of ^{57}Fe. Phys Rev Lett 75: 3545–3548

Hafner S, Raymond M (1967) The nuclear quadrupole coupling tensors of Al^{27} in kyanite. Am Mineral 52: 1632–1642

Hafner SS, Raymond M, Ghose S (1970) Nuclear quadrupole coupling tensors of ^{27}Al in andalusite (Al_2SiO_5). J Chem Phys 52: 6037–6041

Kerrick DM (1990) The Al_2SiO_5 Polymorphs. Reviews in Mineralogy vol. 22. Mineralogical Society of America, Washington DC, pp 37–110

Oganov AR, Brodholt JP (2000) High-pressure phases in the Al_2SiO_5 system and the problem of aluminous phase in the Earth's lower mantle: ab initio calculations. Phys Chem Miner 27: 430–439

Olbricht W, Chatterjee ND, Miller K (1994) Bayes estimation – a novel approach to derivation of internally consistent thermodynamic data for minerals, their uncertainties, and correlations. Phys Chem Miner 21: 36–49

Perdew JP, Wang Y (1992) Accurate and simple analytic representation of the electron-gas correlation energy. Phys Rev B 45: 13244–13249

Perdew JP, Burke S, Ernzerhof M (1996) Generalized gradient approximation made simple. Phys Rev Lett 77: 3865–3868

Pyykkö P (1992) The nuclear quadrupole moments of the 20 first elements: high-precision calculations on atoms and small molecules. Z Naturforsch 47a: 189–196

Ralph RL, Finger LW, Hazen RM, Ghose S (1984) Compressibility and crystal structure of andalusite at high pressure. Am Mineral 69: 513–519

Raymond M (1971) Electric-field-gradient calculations in the aluminum silicates (Al_2SiO_5). Phys Rev B 3: 3692–3701

Raymond M, Hafner SS (1970) Nuclear quadrupole coupling tensors of ^{27}Al in sillimanite (Al_2SiO_5). J Chem Phys 53: 4110–4111

Singh DJ (1991) Ground states properties of lanthanum: treatment of extended core states. Phys Rev B 43: 6388–6392

Schwarz K, Ambrosch-Draxl C, Blaha P (1990) Charge distribution and electric-field gradients in $YBa_2Cu_3O_{7-x}$. Phys Rev B 42: 2051–2061

Winkler B, Blaha P, Schwarz K (1996) Ab initio calculation of electric-field-gradient tensors of forsterite. Am Mineral 91: 545–549

Winter JK, Ghose S (1979) Thermal expansion and high-temperature crystal chemistry of the Al_2SiO_5 polymorphs. Am Mineral 64: 573–586

Yang H, Hazen RM, Finger LW, Prewitt CT, Downs RT (1997a) Compressibility and crystal structure of sillimanite, Al_2SiO_5, at high pressure. Phys Chem Miner 25: 39–47

Yang H, Downs RT, Finger LW, Hazen RM, Prewitt CT (1997b) Compressibility and crystal structure of kyanite, Al_2SiO_5, at high pressure. Am Mineral 82: 467–474